iScience

CellPress
OPEN ACCESS

Article

Role of Fyn and the interleukin-6-STAT-3-autophagy axis in sarcopenia

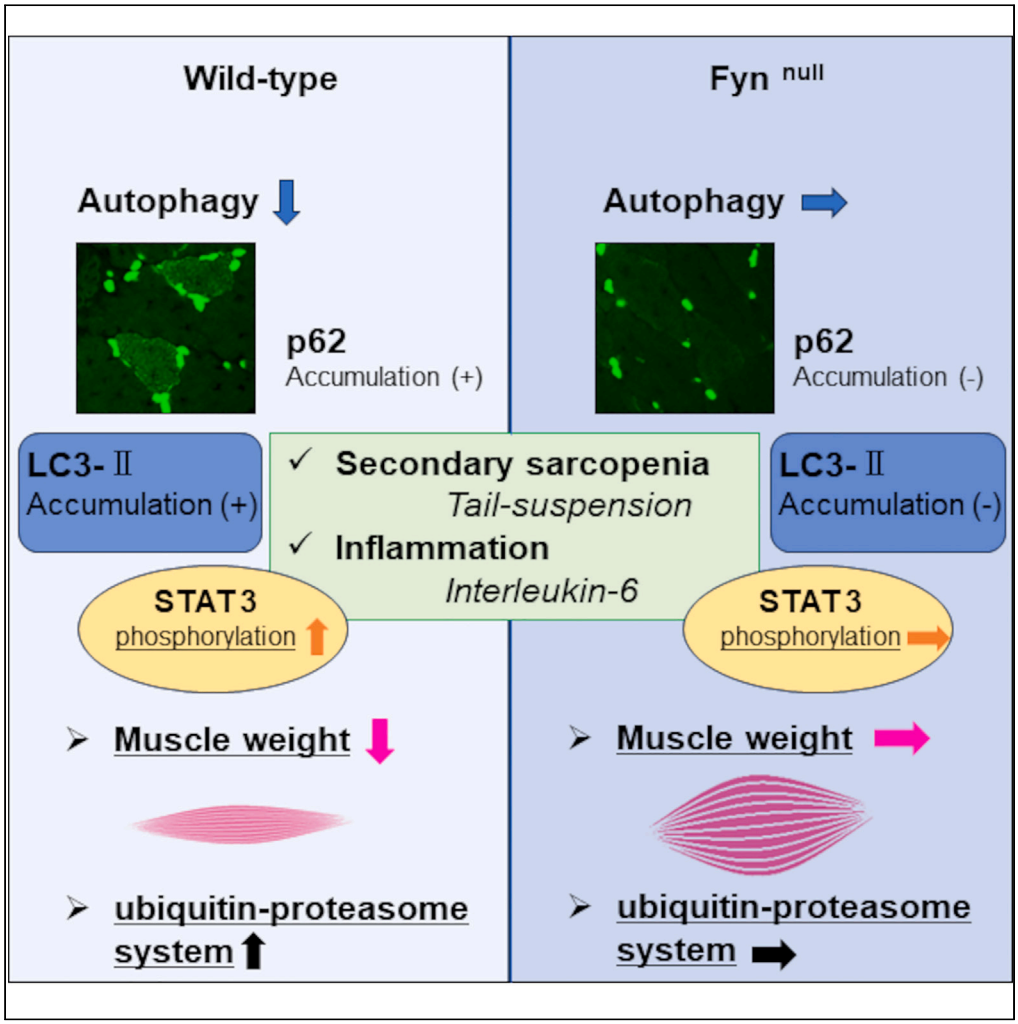

Tsuyoshi Sasaki, Eijiro Yamada, Ryota Uehara, Shuichi Okada, Hirotaka Chikuda, Masanobu Yamada

eijiro.yamada@gunma-u.ac.jp

Highlights

We assessed the role of inflammation in Fyn-STAT3-dependent autophagy & sarcopenia

Fyn was found to be associated with the IL-6-STAT3-autophagy axis in sarcopenia

This finding improves our understanding of sarcopenia-associated metabolic diseases

Sasaki et al., iScience 26, 107717
October 20, 2023 © 2023 The Author(s).
https://doi.org/10.1016/j.isci.2023.107717

iScience

CellPress
OPEN ACCESS

Article

Role of Fyn and the interleukin-6-STAT-3-autophagy axis in sarcopenia

Tsuyoshi Sasaki,[1] Eijiro Yamada,[2,3,*] Ryota Uehara,[2] Shuichi Okada,[2] Hirotaka Chikuda,[1] and Masanobu Yamada[2]

SUMMARY

Sarcopenia is the progressive loss of muscle mass wherein Fyn regulates STAT3 to decrease autophagy. To elucidate the role of inflammation in Fyn-STAT3-dependent autophagy and sarcopenia, here we aimed to investigate the underlying mechanisms using two mouse models of primary and secondary sarcopenia: (1) tail suspension and (2) sciatic denervation. In wild-type mice, the expression of *Fyn* and *IL-6* increased significantly. The expression and phosphorylation levels of STAT3 were also significantly augmented, while autophagic activity was abolished. To investigate Fyn-dependency, we used tail suspension with Fyn-null mice. In tail-suspended wild-type mice, IL-6 expression was increased; however, it was abolished in Fyn-null mice, which maintained autophagy and the expression and ablation of STAT3 phosphorylation. In conclusion, Fyn was found to be associated with the IL-6-STAT3-autophagy axis in sarcopenia. This finding permits a better understanding of sarcopenia-associated metabolic diseases and the possible development of therapeutic interventions.

INTRODUCTION

Sarcopenia is defined as the progressive loss of muscle mass and strength.[1] It is classified into two types: primary sarcopenia, which is caused by age-related loss of muscle mass and secondary sarcopenia, which is caused by non-aging factors, including decreased activity, wasting disease, and malnutrition.[2] Owing to an increase in the aging population in numerous countries, the number of people with sarcopenia worldwide is increasing rapidly.[3] Sarcopenia is reported to lead to metabolic syndrome; it impairs daily activity and is accompanied by a progressive increase in body fat. Skeletal muscle accounts for 40–50% of mammalian tissue and is important for whole-body energy metabolism.[4]

In recent years, autophagy has been reported to be a mechanism responsible for sarcopenia.[5] Originally described as an evolutionarily conserved cellular recycling program,[6] autophagy has recently been implicated in sarcopenia as a cause of various pathophysiologies, such as increased levels of protein aggregates and reactive oxygen species as well as mitochondrial dysfunction.[6] These are hallmarks of inflammatory processes, which suggest that inflammatory molecules modulate autophagy.[7] Tumor necrosis factor alpha (TNFα) and interleukin (IL)-1 and IL-6 have been reported to regulate autophagy and induce sarcopenia.[8,9] The IL-6-signal transducer and activator of transcription (STAT) pathway has been implicated in muscle atrophy[10–12]; however, the molecular mechanisms linking autophagy, immunity, and sarcopenia remain to be elucidated.

We focused on autophagy as a system that can regulate both sarcopenia and metabolic syndrome in skeletal muscle. We previously showed, using transgenic mice that the non-receptor tyrosine kinase Fyn participates in metabolic syndrome and regulates autophagy in sarcopenia by regulating STAT3.[13] Notably, IL-6 has been reported to be a regulator of Fyn in myeloma cells.[14]

In the present study, we aimed to further investigate the role of inflammation in mediating Fyn-STAT3-dependent autophagy and sarcopenia, *in vitro* and *in vivo*, using mouse models encompassing both primary and secondary sarcopenia. We applied tail suspension (TS) or sciatic denervation to young or middle-aged mice. Furthermore, we examined the physiological role of Fyn in regulating autophagy, which leads to sarcopenia. We hypothesized that Fyn is involved in metabolic syndrome and the pathogenesis of sarcopenia. Through this study, we intend to provide a better understanding of the pathology of sarcopenia obesity and enable the development of therapeutic methods.

RESULTS

TS secondary sarcopenia model shows autophagy deficiency mediated by Fyn–STAT3 in mouse muscles

Deficits in autophagy are characteristic of certain sarcopenia models and are reported to result in muscle atrophy.[15,16] To confirm whether autophagy is dysregulated in secondary sarcopenia models, we established a TS mouse model representing disuse-induced muscle atrophy.[17,18] Two weeks after wild-type (WT) mice (8–12 weeks old) were subjected to TS, the weight of all hindlimb muscles, except the extensor digitorum longus and quadriceps, significantly decreased by 10–40%, compared with that in control mice ($p < 0.005$) (Figure 1A). The extensor

[1]Department of Orthopaedic Surgery, Gunma University Graduate School of Medicine, Maebashi, Japan
[2]Department of Internal Medicine, Division of Endocrinology and Metabolism, Gunma University Graduate School of Medicine, Maebashi, Japan
[3]Lead contact
*Correspondence: eijiro.yamada@gunma-u.ac.jp
https://doi.org/10.1016/j.isci.2023.107717

This is an open access article under the CC BY-NC-ND license (http://creativecommons.org/licenses/by-nc-nd/4.0/).

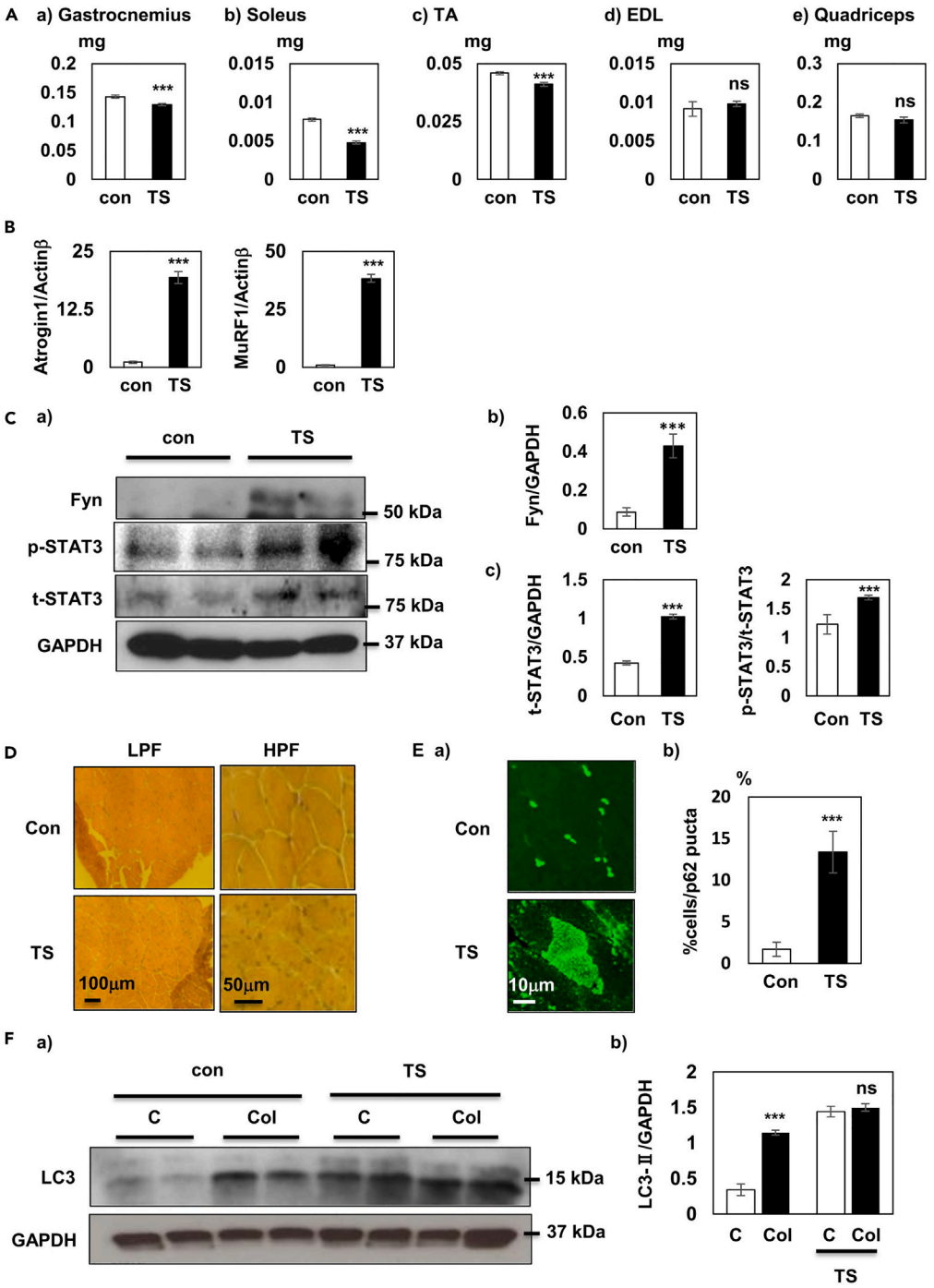

Figure 1. Muscular autophagy in the tail-suspension secondary sarcopenia model

(A) Selective muscle sizes from control and TS mice (n = 6 per group). Data are expressed as mean ± SEM. ***p < 0.005 vs. control.

(B) mRNA expression levels of atrogin-1 and MuRF-1, relative to β-actin, in the gastrocnemius muscles of TS mice (n = 3). Data are expressed as mean ± SEM. ***p < 0.005 vs. control.

(C) Representative immunoblots from three independent experiments with gastrocnemius muscles of control and TS mice, developed using the indicated antibodies. Signal quantification of the protein expression levels of Fyn, normalized to GAPDH (n = 3). Data are shown as mean ± SEM. ***p < 0.005 vs. control. Signal quantification of the expression levels of total STAT3, normalized to GAPDH, and phosphoY705-STAT3, normalized with total STAT3 (n = 3). Data are shown as mean ± SEM. ***p < 0.005 vs. control.

(D) Representative H&E staining of control and TS mice. See also Figure S2.

Figure 1. *Continued*

(E) Representative p62 immunofluorescence visualized in control and TS mice. Proportion of p62-positive myocytes in control and TS mice (n = 3). Data are expressed as mean ± SEM. *p < 0.05 vs. control.

(F) Three-month-old control and TS mice were treated with either vehicle (as control) or 0.4 mg/kg/day colchicine for two days. Immunoblots of the TA muscle were obtained using the indicated antibodies. Representative immunoblots of three independent experiments. Signal quantification of the expression levels of LC3-II, normalized with GAPDH levels (n = 3). Data are expressed as mean ± SEM. ***p < 0.005 vs. control. The Mann–Whitney U test was used for statistical comparison. The bars on each column show standard error of the mean. Scale bars in the tissue images represent the lengths defined in each figure. Abbreviations: TA, tibialis anterior; TS, tail suspension; SEM, standard error of the mean; GAPDH, glyceraldehyde 3-phosphate dehydrogenase; STAT3, signal transducer and activator of transcription 3; C, control; Col, colchicine.

digitorum longus is primarily composed of glycolytic (white) muscle fibers, whereas the other skeletal muscles are mostly composed of oxidative (red) muscle fibers (e.g., the soleus) or a mixture of oxidative and glycolytic muscle fibers (e.g., the gastrocnemius, tibialis anterior, and quadriceps). The weight of soleus muscles decreased the most (40%), which indicated that red muscle was the most affected by TS. The protein level of ubiquitin ligases atrogin-1 and MuRF-1, which are markers of muscle loss, was increased in the muscles of TS mice compared with that in controls ($p < 0.005$) (Figure 1B).[19] Because coordination of Fyn-STAT3-autophagy regulates muscle mass,[13] we examined the expression level of *Fyn*. It was significantly increased in the muscles of TS mice, compared with that in controls ($p < 0.005$) (Figure 1C). Moreover, there was a significant increase in STAT3 protein levels and in phosphorylation at tyrosine 705, which is indispensable for its transcriptional activation and could be regulated by Fyn[13] ($p < 0.005$) (Figure 1C). This indicates that Fyn-STAT3 is an important target in models of secondary sarcopenia. Autophagy deficits result in decreased muscle mass and inflammation, with myocytes characterized by reduced size and small, central nuclei.[16] Histological analysis of the gastrocnemius muscle using hematoxylin and eosin (H&E) staining revealed a reduction in muscle fiber size, with fibers displaying phenotypic characteristics of muscle degeneration, such as central nuclei, nuclear hypertrophy, elongated nuclei, and myofibril vacuoles, indicating autophagy deficits (Figure 1D and Figure S2).

To evaluate autophagic activity in the skeletal muscle of a secondary sarcopenia model, we evaluated the expression levels of p62, a protein consumed by autophagy, and LC3-II, which indicates the autophagosome level.[6] p62 is an adapter protein that binds autophagosomes to degradation substrates; this is degraded through autophagy.[6] With reduced autophagic activity, p62 is not degraded and instead accumulates.[6] LC3-II is expressed on the inner and outer membranes of the autophagosome bilayer; it is expressed on the inner membrane and degrades as autophagy proceeds.[6,15] LC3-II expression indicates the amount of autophagosome present. Although its level increases (accumulates) with the administration of autophagosome-degradation inhibitors when autophagy is in progress, it does not accumulate when autophagy is reduced.[15] The change in LC3-II expression after administration of an autophagosome-degradation inhibitor enables direct evaluation of autophagic activity (autophagy flux assay).[15,20] In this study, quantitative evaluation of LC3 was performed by assessing the expression of LC3-II (as described in the STAR Methods) and comparing the difference in expression between the control and intervention groups with and without autophagosome-degradation inhibitors.

SQSTM1/p62 immunofluorescence and quantification of autophagic vacuoles in the TA muscles of TS mice showed a perturbation of muscular macroautophagy compared with that in control mice ($p < 0.005$) (Figure 1E). An *in vivo* autophagy flux assay was performed to compare the expression of LC3-II in untreated mice and mice treated with the autophagosome-degradation inhibitor colchicine, as reported previously.[15] In control mice, colchicine treatment led to an increase in LC3-II protein levels ($p < 0.005$), indicating the occurrence of autophagy. Relatively few changes were observed in TS mice (Figure 1F), indicating autophagy deficits in TS mouse muscles.

Denervation secondary sarcopenia models also show autophagy deficits mediated by Fyn-STAT3 in mouse muscles

To determine whether these findings can be generalized across different secondary sarcopenia etiologies, we introduced the denervation mouse model, in which the sciatic nerve was surgically excised, promoting muscle atrophy through disuse or acetylcholine blockade.[21] Atrophy was observed in all denervated muscles and compared with sham operation ($p < 0.005$), except for the quadriceps (Figure S1A). Protein levels of atrogin-1 and MuRF-1 in muscles increased in the denervated mice compared with those in the sham group ($p < 0.005$) (Figure S1B), along with the protein levels of Fyn ($p < 0.005$) (Figure S1C), similar to those in the TS mice (Figure S1C). An increase in STAT3 expression and phosphorylation at tyrosine 705 was observed, similar to that in TS mice (Figure S1C). Autophagic activity, examined via intraperitoneal administration of colchicine, decreased in the muscles of denervated mice, compared with that in the sham group ($p < 0.05$) (Figure S1D). In both secondary sarcopenia models, we found elevated muscular expression of IL-6 compared to that in the control group ($p < 0.05$) (Figure S1E). IL-6 is an inflammatory cytokine upregulated in sarcopenia and involved in its development.[8] TS and denervated mice showed the same characteristics in terms of the Fyn-STAT3-autophagy axis, possibly mediated by IL-6.

IL-6 is involved in Fyn-STAT3 signaling

Inflammatory cytokines, including IL-6, negatively regulate skeletal muscle mass.[8] Previous studies have shown that IL-6 regulates both Fyn and STAT3.[10,14] Because older adults are more likely to develop chronic inflammation, we treated C2C12 cells with IL-1β, IL-6, and IL-18 to examine their effects on the regulation of Fyn–STAT3 signaling in muscular autophagy. Among the cytokines tested, IL-6 alone caused an increase in the level of phosphorylated STAT3 in both myoblasts and myotubes. Fyn expression was higher in myotubes than in myoblasts, indicating that the effect of IL-6 on STAT3 phosphorylation is dependent on Fyn and is stronger in myotubes than in myoblasts (Figure 2A).

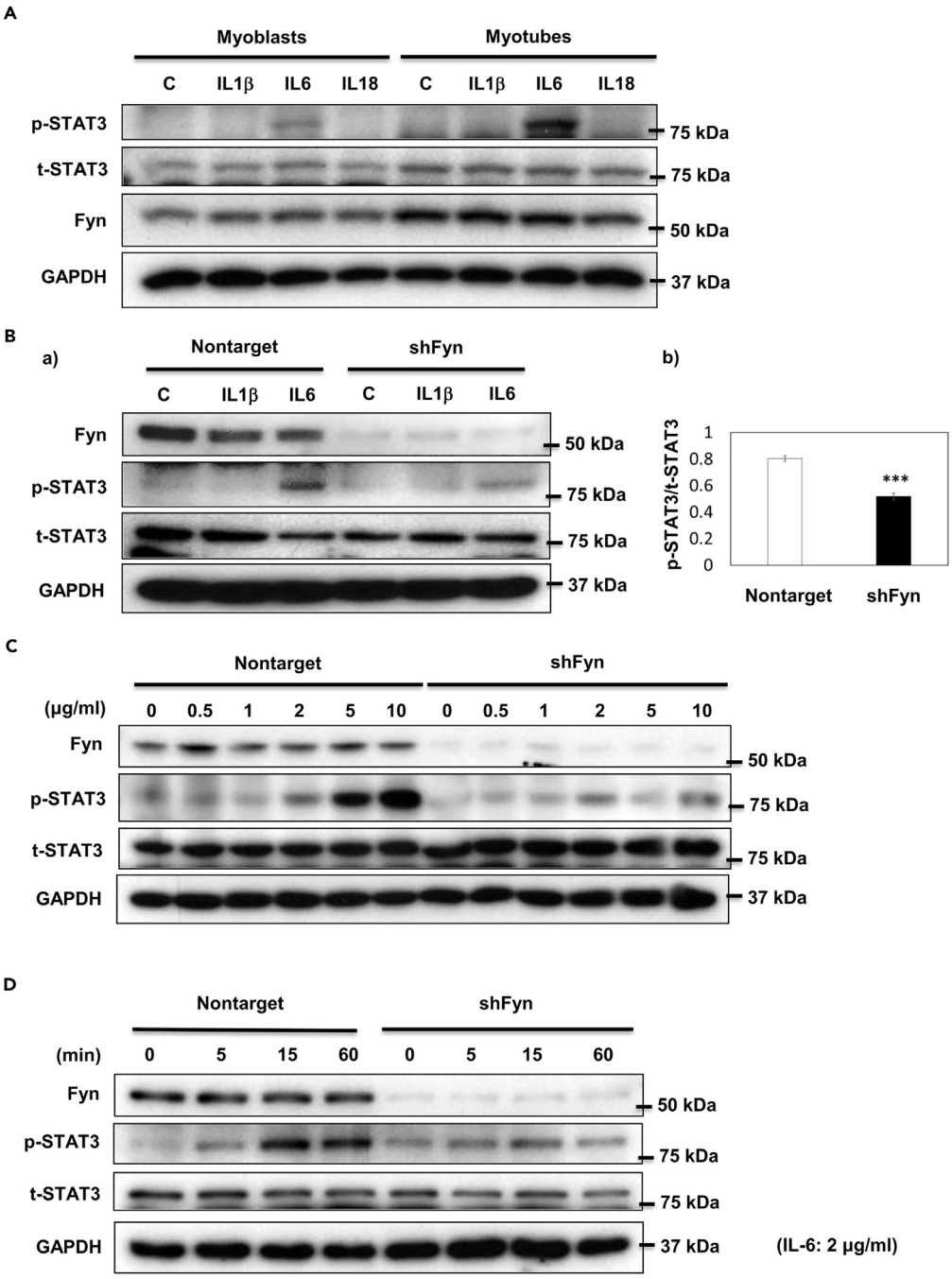

Figure 2. Analysis of upstream activators of Fyn for STAT3 in C2C12 cells

(A) Representative immunoblots from three independent experiments on lysates of C2C12 myoblasts and myotubes developed using the indicated antibodies.

(B) C2C12 myotubes expressing either non-target or Fyn shRNA were developed using the indicated antibodies (a). Signal quantification of the expression levels of phosphoY705-STAT3 induced by IL-6 treatment, normalized to total STAT3 (n = 3). Data are expressed as mean ± SEM. ***p < 0.001 vs. non-target (b). The Mann-Whitney U test was used for statistical comparison.

(C) IL-6 dose dependency on phosphorylation of STAT3 in C2C12 myotubes expressing either non-target or Fyn shRNA.

(D) Time dependency of IL-6 treatment on phosphorylation of STAT3 in C2C12 myotubes expressing either non-target or Fyn shRNA. The bars on each column show standard error of the mean. Abbreviations: STAT3, signal transducer and activator of transcription 3; IL-6, interleukin 6.

To investigate whether IL-6-induced STAT3 phosphorylation is Fyn-dependent, we used shRNA technology to knock down Fyn in C2C12 cells, which was approximately 95% efficient (Figure 2B). IL-6 increased the level of phospho-STAT3 in C2C12 myotubes expressing both non-target and Fyn shRNA. The levels of phospho-STAT3 were significantly decreased in C2C12 cells expressing Fyn shRNA, indicating that STAT3 phosphorylation is mostly Fyn-dependent ($p < 0.001$) (Figure 2B). To confirm this, we performed a dose-response and time-course study. STAT3 phosphorylation was enhanced by IL-6 in a dose-dependent manner in C2C12 cells expressing non-target shRNA, whereas no dose-dependent enhancement of STAT3 phosphorylation was observed in C2C12 cells expressing Fyn shRNA (Figure 2C). Similarly, with time, STAT3 phosphorylation was enhanced in C2C12 cells expressing non-target shRNA in response to IL-6 exposure. However, there was relatively less time-dependent enhancement of phosphorylation in C2C12 cells that expressed Fyn shRNA, which confirmed that STAT3 phosphorylation by IL-6 was Fyn-dependent (Figure 2D).

IL-6 regulates STAT3 and autophagy in myotubes via Fyn

Although we identified Fyn and STAT3 as targets of IL-6, the underlying mechanism remained unclear. Therefore, we examined whether Fyn is activated by IL-6. The expression of Fyn did not change after IL-6 treatment; however, IL-6 treatment induced the phosphorylation of tyrosine 417, which is located in the kinase domain and is indispensable for Fyn activity (Figure 3A). Co-immunoprecipitation of Fyn and STAT3 in IL-6-treated C2C12 cells revealed that they formed a complex that shows increased levels in C2C12 myotubes upon IL-6 treatment (Figure 3B). Taken together, these data confirm the existence of the IL-6-Fyn-STAT3 axis. Furthermore, a possible mechanism of Fyn-dependent STAT3 phosphorylation is indicated.

Because the regulation of autophagy by Fyn-STAT3 is supported by a previous report,[13] as well as the data from our secondary sarcopenia models, we examined the role of IL-6 in this mechanism. We assessed autophagy flux by comparing the expression of LC3-II in C2C12 myotubes cultured with or without the autophagosome-degradation inhibitor ammonium chloride/leupeptin, as reported previously.[22]

In non-target C2C12 cells, the expression of LC3-II did not change with ammonium chloride/leupeptin treatment following administration of IL-6, showing downregulation of autophagosome turn-over and indicating decreased autophagy flux (Figure 4C). However, in C2C12 cells expressing Fyn shRNA, the expression of LC3-II was upregulated by ammonium chloride/leupeptin treatment even after IL-6 administration, indicating that Fyn knockdown rescued the decay of autophagic flow induced by IL-6 in C2C12 myotubes (Figures 4C and 4D). IL-6 was shown to downregulate autophagy flux, and Fyn was shown to be a negative regulator of autophagy in C2C12 myotubes.

A Fyn-knockout mouse model confirms the role of Fyn in sarcopenia

To confirm whether Fyn dysregulates autophagy in secondary sarcopenia, we subjected 12-month-old Fyn-null mice to TS to induce muscle atrophy. Two weeks after WT mice were subjected to TS, their hindlimb muscle weight decreased significantly by 5–45% compared to that of the controls ($p < 0.005$) (Figure 4A). Although older mice showed this decrease in all muscles, in younger mice, the extensor digitorum longus and quadriceps muscles were resistant to sarcopenia (Figure 1A). Notably, all muscles of Fyn-null mice were resistant to TS-induced sarcopenia. Two-way ANOVA was conducted to determine whether sarcopenia resistance was characterized by Fyn knockout compared with C57/B6N wild-type mice. The results showed that sarcopenia resistance was associated with Fyn knockout in gastro, TA, and quadriceps ($p < 0.05$) but not in Soleus or EDL. For Soleus and EDL, muscle atrophy tended to be rescued by Fyn knockout; however, this result was not significant, as indicated by two-way ANOVA. This may be because the muscles themselves are smaller; hence, the changes in muscle mass are smaller and experimentally less different. Alternatively, the regulation of Fyn may be critical in muscle mass atrophy, especially in relatively larger skeletal muscles.

Cytochrome *c* oxidase (COX) and succinate dehydrogenase (SDH) staining indicated an increase in mitochondrial function in the TA muscles of WT mice subjected to TS (Figure 5 and Figure S3). This has been observed in other skeletal muscle myopathies that have compromised autophagic function, such as Danon and X-linked myopathy.[23] However, no significant differences were observed in the muscles of Fyn-null mice subjected to TS. Glycogen levels around the nucleus and in the cytoplasm were elevated in the muscles of WT mice subjected to TS; however, this was not observed in the muscles of Fyn-null mice (Figure 5). Glycogen is a known substrate for autophagy, indicating that autophagy may have been inhibited by TS. However, glycogen levels are not solely controlled by autophagy, and the influence of other factors cannot be excluded. Increased sarcoplasmic or endoplasmic reticulum Ca^{2+} ATPase-1 (SERCA1) positivity for type 2 muscle fibers and decreased SERCA2 positivity for type 1 muscle fibers demonstrated the occurrence of a class switch in the muscles of WT mice subjected to TS and indicated the inhibition of autophagy. This was not observed in the muscles of Fyn-null mice subjected to TS (Figure S4). Moreover, nicotinamide adenine dinucleotide tetrazolium reductase (NADH-TR) staining demonstrated insufficient staining of the intermyofibrillar network between atrophied myofibers in WT mice subjected to TS. This was not observed in Fyn-null mice subjected to TS, which indicates that the muscles of Fyn-knockout mice possess both qualitative and quantitative preventive mechanisms against TS-induced muscular atrophy (Figure S5).

The levels of atrogin-1 and MuRF-1 increased in the muscles of WT mice subjected to TS, compared with those in controls ($p < 0.05$) but not in Fyn-null mice subjected to TS. This suggests that Fyn-null mice are resistant to sarcopenia (Figure 4B). Moreover, STAT3 phosphorylation at tyrosine 705 was reduced in the muscles of Fyn-null TS mice compared to that in WT mice subjected to TS ($p < 0.005$); however, the expression levels of STAT3 did not change. This supports the proposition that Fyn-STAT3 is an important target for sarcopenia (Figure 4C). Finally, the mRNA levels of IL-6 increased in the muscles of WT mice subjected to TS; however, the gene expression level of IL-6 did not change in Fyn-null mouse sarcopenia models (Figure 4D).

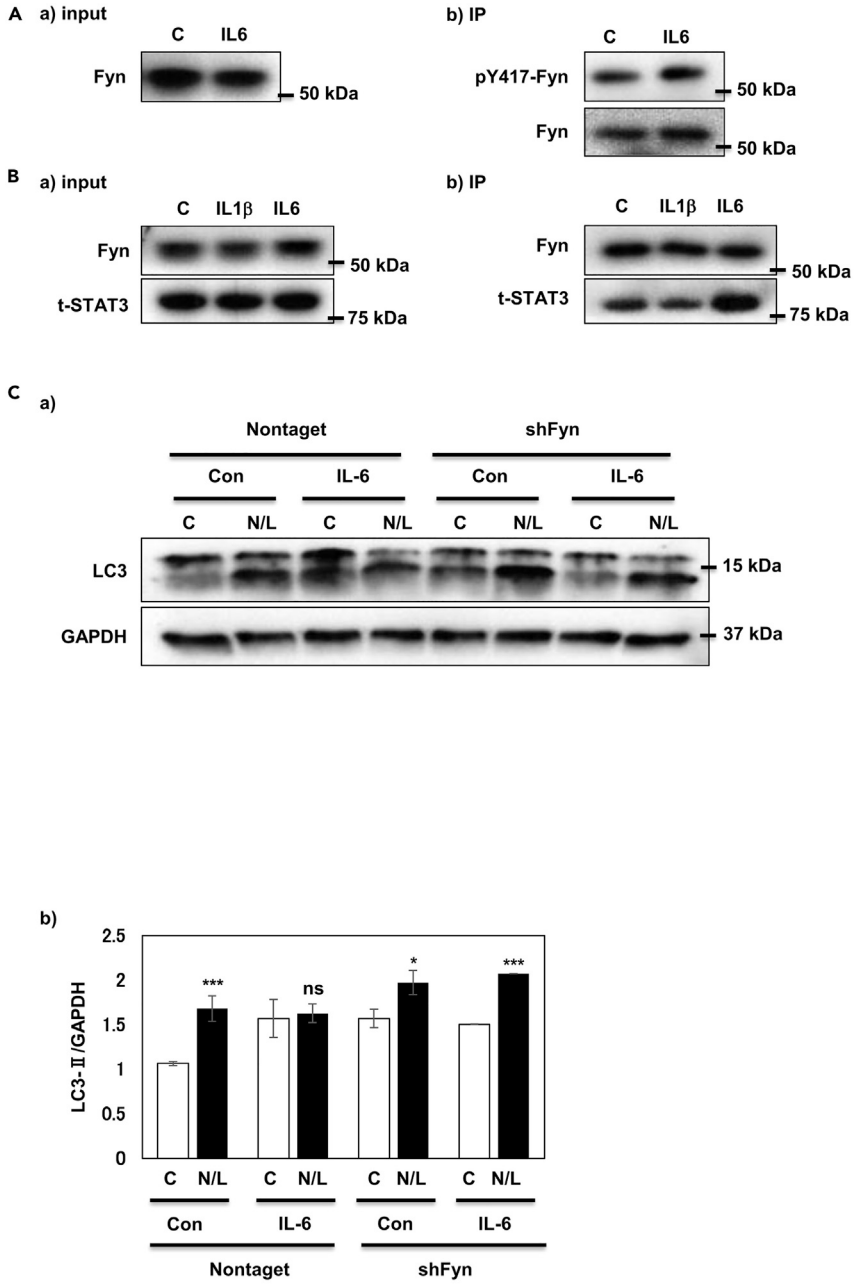

Figure 3. Fyn-dependent STAT3 regulation of autophagy

(A) Representative immunoblots from three independent experiments. After 15 min of IL-6 treatment, lysates of C2C12 myotubes were immunoprecipitated with Fyn antibody and immunoblots were prepared using the indicated antibodies.

(B) Representative immunoblots from three independent experiments. After 15 min of either IL-1β or IL-6 treatment, lysates of C2C12 myotubes were immunoprecipitated with total STAT3 antibody, followed by immunoblotting with Fyn.

(C) Representative immunoblots from three independent experiments indicating autophagy flux in myotube lysates, determined after NH_4Cl/leupeptin treatment for 2 h, followed by IL-6 treatment. Lysates were immunoblotted with the indicated antibodies (a). Signal quantification of the expression levels for LC3-II, normalized to GAPDH (n = 3) (b). Data are expressed as mean ± SEM. *p < 0.05, ***p < 0.005 vs. control. The Mann-Whitney U test was used for statistical comparison. The bars on each column show standard error of the mean. Abbreviations: STAT3, signal transducer and activator of transcription; IL, interleukin; GAPDH, glyceraldehyde 3-phosphate dehydrogenase; SEM, standard error of the mean; N/L, NH_4Cl/leupeptin.

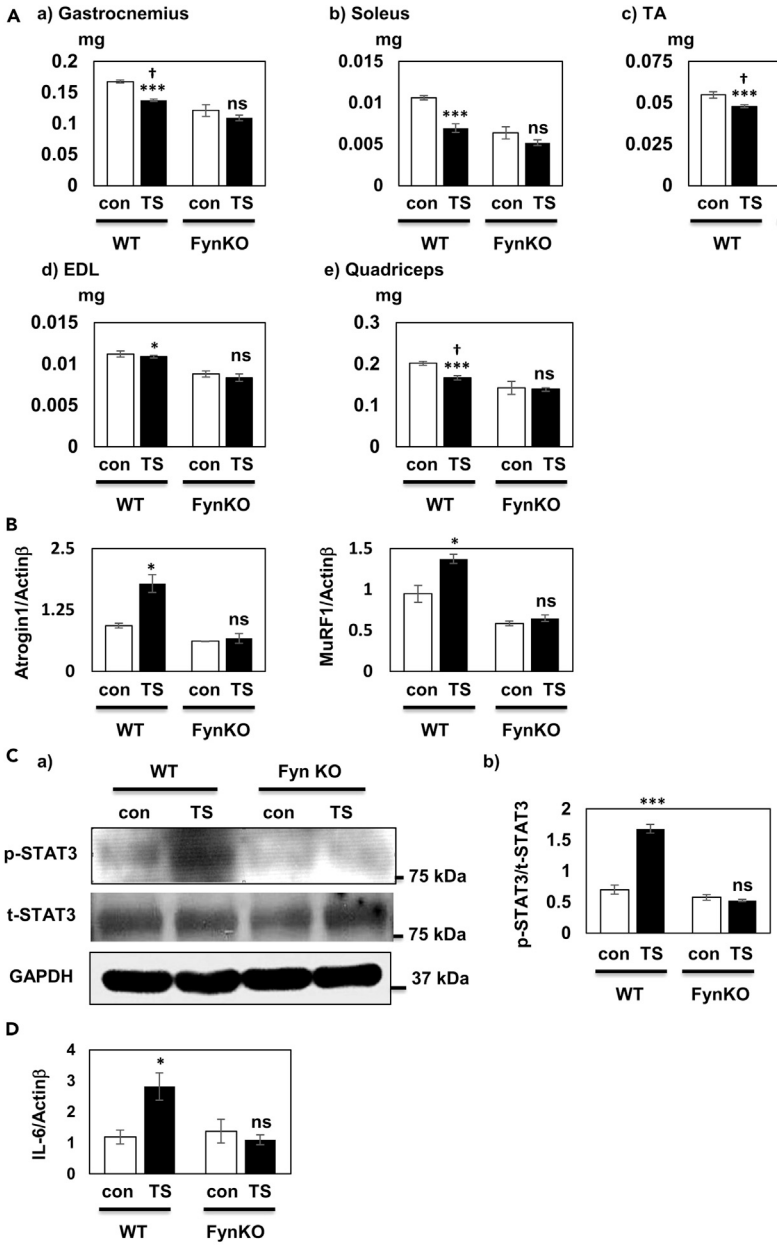

Figure 4. Fyn–STAT3-dependent sarcopenia

(A) Selective muscle sizes of WT and Fyn-KO mice in the control and TS groups (n = 6 per group). Data are expressed as mean ± SEM. ***p < 0.005 vs. WT.

(B) mRNA expression levels of atrogin-1 and MuRF-1, relative to β-actin, in the gastrocnemius muscles of WT and Fyn-KO mice with TS vs. controls (n = 3). Data are expressed as mean ± SEM. ***p < 0.005 vs. WT.

(C) Immunoblots of gastrocnemius muscles of WT and Fyn-KO mice (TS and control) were developed using the indicated antibodies. Signal quantification of the expression levels for phosphoY705–STAT3, normalized to total STAT3 (n = 3). Data are expressed as mean ± SEM. ***p < 0.005 vs. WT.

(D) mRNA expression levels of IL-6, relative to β-actin, in the gastrocnemius muscles of WT and Fyn-KO mice (TS or control) (n = 3). Data are expressed as mean ± SEM. ***p < 0.005 vs. WT. The Mann–Whitney U test was used for statistical comparison. The bars on each column show standard error of the mean. Abbreviations: WT, wild-type; Fyn-KO, Fyn-knockout; SEM, standard error of the mean; STAT3, signal transducer and activator of transcription 3; IL-6, interleukin 6.

As described previously, histological analyses of the muscles of WT mice subjected to TS revealed a remarkable reduction in the size of muscle fibers and phenotypic characteristics of muscle degeneration, including nuclear hypertrophy, elongated nuclei, and myofibril vacuoles, which together indicate autophagy deficits (Figures 1D and 6A).[16,24] In contrast, the muscles of Fyn-null mice showed no remarkable changes after TS, which confirmed that they were resistant to TS-induced sarcopenia (Figure 6A). In WT mice, TS caused a leftward shift in

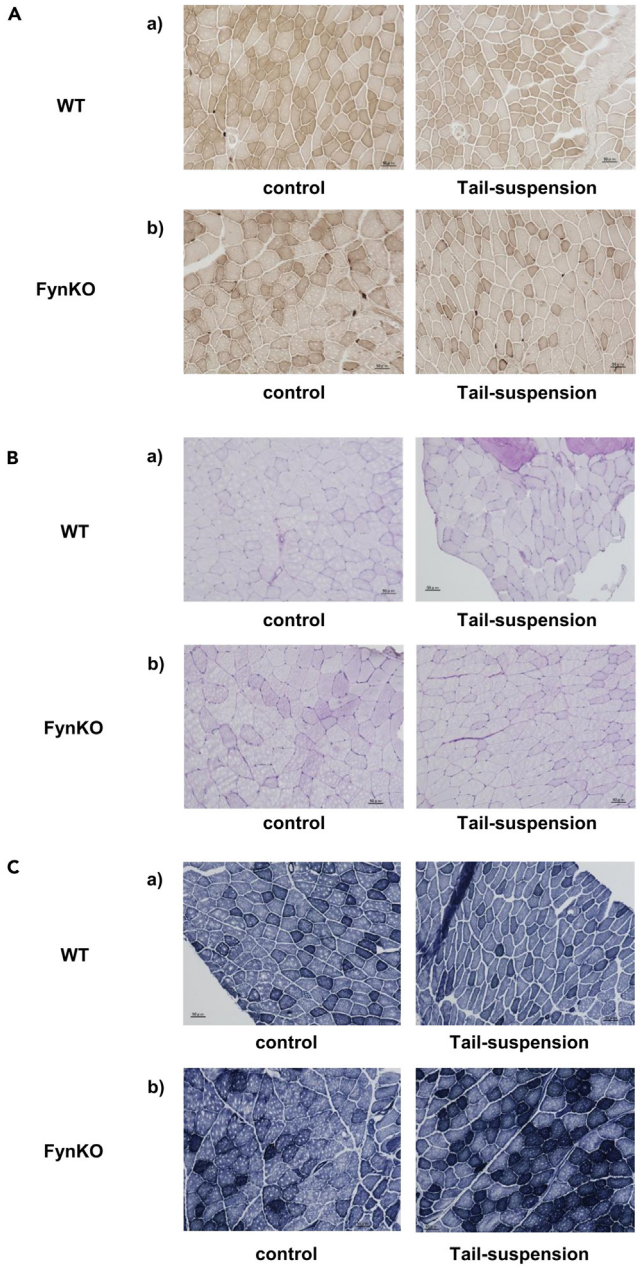

Figure 5. COX, PAS, and NADH-TR staining of the TA muscles of tail-suspended mice

(A) COX staining demonstrates a marked increase in the number of mitochondria in the TA muscles of WT mice subjected to TS (a), whereas no significant differences are observed in the muscles of Fyn-null mice subjected to TS (b).

(B) The level of perinuclear and cytoplasmic glycogen, a known substrate of autophagy, is increased in the muscles of WT mice subjected to TS (a), indicating the inhibition of autophagy, which is not observed in the muscles of Fyn-null mice subjected to TS (b).

(C) NADH-TR staining demonstrates a decrease in the cross-sectional area of type 2 muscle fiber (light-stained fibers) size in the TA muscles of WT mice subjected to TS (a), whereas no significant differences are observed in the muscles of Fyn-null mice subjected to TS (b). See also Figure S5. Scale bars in the tissue images represent the lengths defined in each figure.

the distribution of muscle cross-sectional area (reduced cross-sectional area). However, there was less variation in the distribution of muscle cross-sectional area in knockout mice due to TS (Figure 6B). Analyses of muscle cell size revealed that the mean cross-sectional area of type 2 muscle fibers significantly decreased after TS in WT mice (control: 2034.4 (SD 304.9), TS: 1677.7 (SD 282.6) μm^2, $p < 0.001$); there were no significant changes in Fyn-null mice (control: 2941.2 (SD 666.6), TS: 3165.8 (SD718.4) μm^2, $p = 0.122$), indicating that they were resistant to TS-induced sarcopenia (Figure 6B). Although a perturbation of muscle macroautophagy was observed (based on SQSTM1/p62

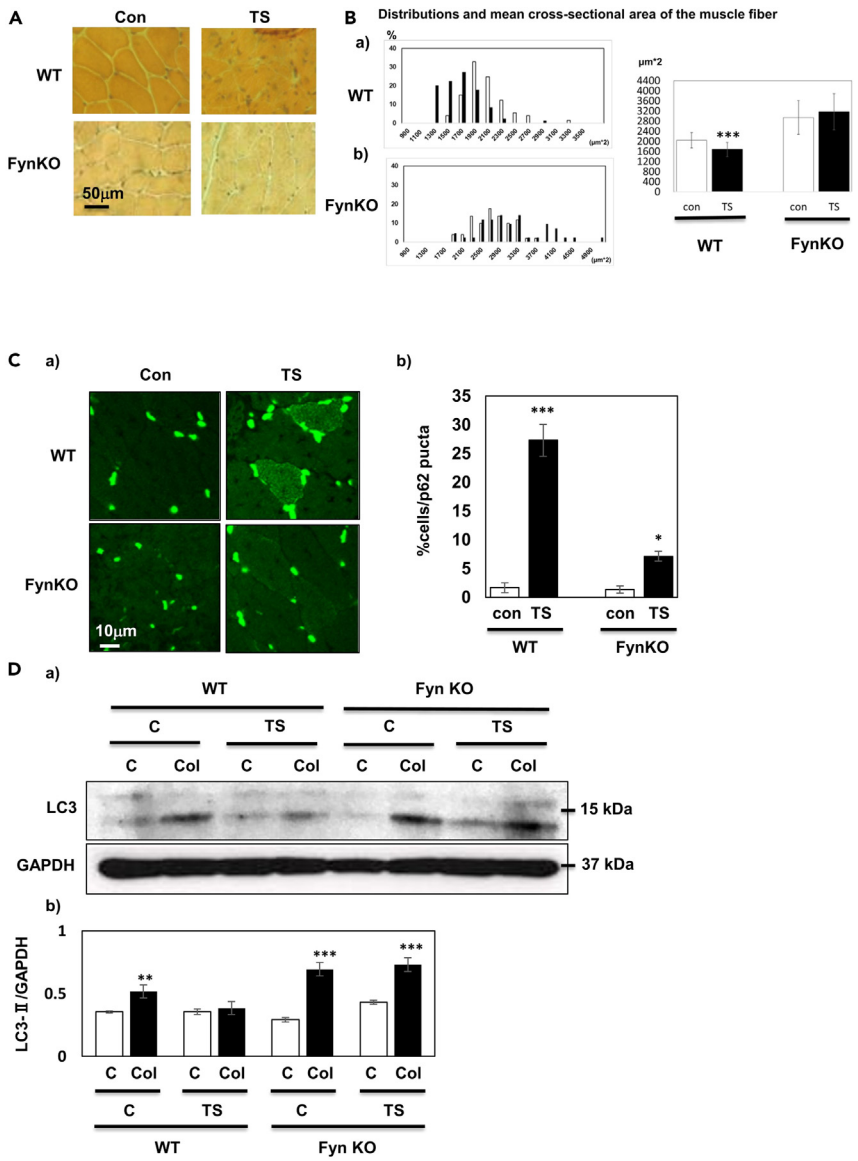

Figure 6. Fyn-dependent autophagy in muscles with sarcopenia

(A) Representative H&E staining of WT and Fyn-KO mice (TS and control).

(B) The size distribution of myofibers of WT (upper panel) and Fyn-KO (lower panel) mice with TS (black bar) or control (white bar).

(C) Representative p62 immunofluorescence visualized in WT and Fyn-KO mice (TS and control). Proportion of p62-positive myocytes of WT and Fyn-KO mice (TS and control; n = 3). Data are expressed as mean ± SEM. *p < 0.05 vs. control.

(D) Representative immunoblots from three independent experiments where lysates of three-month-old control and TS mice were treated with either vehicle or 0.4 mg/kg/day colchicine for two days and TA tissues were immunoblotted with the indicated antibodies. Signal quantification of the expression levels of LC3-II, normalized to GAPDH (n = 3). Data are expressed as mean ± SEM. *p < 0.05 vs. control. The Mann–Whitney U test was used for statistical comparison between groups. The bars on each column show standard error of the mean. Scale bars in the tissue images represent the lengths defined in each figure. Abbreviations: H&E, hematoxylin & eosin; WT, wild-type; Fyn-KO, Fyn knockout; TS, tail suspension; SEM, standard error of the mean; TA, tibialis anterior; GAPDH, glyceraldehyde 3-phosphate dehydrogenase. C, control, Col, colchicine.

immunofluorescence and the quantification of autophagic vacuoles in the muscles of WT mice) (Figure 6C), no remarkable change was observed in the muscles of Fyn-null mice. Finally, an *in vivo* autophagy flux assay was performed (Figure 6D). In control WT mice, an increase in LC3-II protein level was observed after colchicine treatment, indicating that autophagy existed; however, relatively few changes were observed in tail-suspended WT and Fyn-null mice, which indicated that the TS-induced deficits of autophagy in WT mice were rescued in the muscles of Fyn-null mice.

DISCUSSION

Skeletal muscle atrophy is a major challenge in the health of an aging population.[25] Therefore, to understand the pathogenesis of muscle atrophy, the development of appropriate mouse models has become increasingly important.[26] Various methods have been used to induce muscle atrophy, including aging, cast fixation, denervation, hindlimb suspension, and immobilization using splints, staples, or spiral wires.[27] External fixation methods (e.g., cast fixation) are most commonly used in mouse models of secondary sarcopenia because they are practical and are used in clinical practice.[27] However, external fixation methods can cause adverse events, such as edema, necrosis, and skin damage, which are health-affecting factors not related to muscular disuse.[27] In this study, we used a sciatic denervation model and a hindlimb non-load model as secondary sarcopenia models. To investigate the role of Fyn in sarcopenia, we used the TS model with Fyn-null mice because the denervation model could mediate sarcopenia by modifying the neuromuscular junction assembly, especially the acetylcholine receptor,[21] which is reported to bind to and is regulated by Fyn.[28] We used middle-aged mice (aged 12 months) to accelerate sarcopenia because older mice are reported to have primary sarcopenia characteristics, which include major phenotypes, such as loss of muscle fiber cross-sectional area and muscle mass, along with molecular mechanisms, such as increased oxidative stress, mitochondrial dysfunction, and levels of MuRF1 and atrogin-1, and decreased protein synthesis, Akt/p70S6K signaling, and IGF-1 signaling.[29] We found that middle-aged Fyn-null mice showed resistance to secondary sarcopenia through the IL-6-Fyn-STAT3-autophagy axis. Fyn-null mice were resistant to the class switch of muscle fiber types, an important aspect of sarcopenia that has been observed in several mouse models.

Studies have been conducted to explore the relationship between autophagy and muscle atrophy. You et al.[30] reported that autophagy acts as a protective factor against skeletal muscle regeneration after trauma and age-related skeletal muscle weakness. Nascimbeni et al.[31] reported that decreased autophagy leads to skeletal muscle atrophy in glycogen storage disease. These reports suggest that proper function of autophagy is important for the maintenance and regeneration of skeletal muscles. In this study, we found that non-weight-bearing by TS caused a decrease in lower limb skeletal muscle weight and autophagy function in skeletal muscles, which were rescued by Fyn knockout. The maintenance of autophagy was associated with the prevention of non-weight-bearing muscle weight loss. Our results are consistent with those of previous studies showing that autophagy has a positive role in maintaining skeletal muscle mass. The upstream molecules and mechanisms that underlie the autophagic regulation of sarcopenia remain unknown. Inflammation can link autophagy and sarcopenia in this regard, as it can mediate the sharing of major characteristics and molecular mechanisms.[7] Indeed, the levels of proinflammatory cytokines (e.g., TNFα, IL-1, and IL-2) have been reported to increase during aging and regulate sarcopenia.[32,33] IL-6 has multifunctional and intricate roles in muscles;[34] it not only mediates muscular metabolism but also promotes muscle hypertrophy and atrophy.[8,34] Notably, there is controversy regarding reports on circulating IL-6 levels in sarcopenia.[35] We found that IL-6 levels were elevated locally in the muscles of primary sarcopenia models, which might directly influence muscle inflammation and regulate muscle mass. It has been reported that IL-6 mediates the JAK–STAT3 pathway to regulate muscle mass; however, there are few reports on its role in autophagy.[11,12] The relationship between Fyn and IL-6 in muscle has been previously described only in one study related to muscle differentiation.[36] Here, we confirmed that the Fyn-dependent IL-6-STAT3-autophagy pathway can regulate sarcopenia. Further studies are required to investigate the role of Fyn in the JAK-STAT3 pathway, especially with regard to autophagy.

The role of Fyn in STAT3 regulation has been established in many reports; however, the underlying molecular mechanisms by which Fyn regulates STAT3 expression and phosphorylation remain unclear.[13,37] In this study, we found that Fyn could bind to STAT3. Interestingly, the level of Fyn-STAT3 complex was increased by IL-6 but not by IL-1β (a proinflammatory cytokine that mediates sarcopenia), which highlights the importance of IL-6 in STAT3 regulation in sarcopenia. Further studies are necessary to identify the binding mechanism and its contribution to STAT3 phosphorylation, especially to determine if the process is direct or indirect.

We utilized conventional Fyn-knockout mice in which Fyn was knocked down in every tissue. Therefore, the developmental aspect of sarcopenia could not be assessed. Hence, the role of Fyn in myocytes remains unclear. Fyn is known to be expressed by inflammatory cells, such as T cells and macrophages, which have important roles in muscle inflammation and sarcopenia.[38] Muscle atrophy could be induced by satellite cell dysfunction in mediating the differentiation of myoblasts into myotubes.[39] Further myocyte-specific Fyn-null studies or time-dependent induced Fyn-null mouse models are necessary. Nevertheless, in summary, we identified the physiological role of Fyn in sarcopenia, the regulation of which is mediated by IL-6-dependent STAT3 phosphorylation and autophagy. This study indicated the possible role of Fyn in sarcopenia. An improved understanding of the mechanisms underlying sarcopenia can lead to the development of new therapeutic modalities.

Limitations of the study

There are several limitations to this study. First, although Fyn-knockout mice were used in the *in vivo* experiments, it is not possible to determine whether the mechanism by which Fyn knockout confers resistance to disuse-induced atrophy is via local effects or systemic effects on the muscle. Second, the disuse-induced atrophy model has not been examined over a time course, making it difficult to examine the causal relationship between the changes in muscle mass and changes in autophagy. However, this study is important because it showed that the tyrosine kinase Fyn is involved in the regulation of muscle mass via autophagy in skeletal muscle using a physiological mode.

STAR★METHODS

Detailed methods are provided in the online version of this paper and include the following:

- KEY RESOURCES TABLE

SUPPLEMENTAL INFORMATION

Supplemental information can be found online at https://doi.org/10.1016/j.isci.2023.107717.

ACKNOWLEDGMENTS

This work was supported by Grants-in-Aid for Scientific Research KAKENHI (20K19705).

AUTHOR CONTRIBUTIONS

E.Y. conceived, designed, and performed the experiments, analyzed the data, and wrote the paper. T.S. performed the experiments, analyzed the data, and wrote the paper. R.U., S.O., H.C., and M.Y. analyzed the data.

DECLARATION OF INTERESTS

The authors declare no competing interests.

Received: January 3, 2023
Revised: July 31, 2023
Accepted: August 22, 2023
Published: August 25, 2023

REFERENCES

1. Morley, J.E., Baumgartner, R.N., Roubenoff, R., Mayer, J., and Nair, K.S. (2001). J. Lab. Clin. Med. *137*, 231–243. https://doi.org/10.1067/mlc.2001.113504.
2. Supriya, R., Singh, K.P., Gao, Y., Li, F., Dutheil, F., and Baker, J.S. (2021). A multifactorial approach for sarcopenia assessment: A literature review. Biology *10*, 1354. https://doi.org/10.3390/biology10121354.
3. Sato, P.H.R., Ferreira, A.A., and Rosado, E.L. (2020). The prevalence and risk factors for sarcopenia in older adults and long-living older adults. Arch. Gerontol. Geriatr. *89*, 104089. https://doi.org/10.1016/j.archger.2020.104089.
4. Nishikawa, H., Asai, A., Fukunishi, S., Nishiguchi, S., and Higuchi, K. (2021). Metabolic syndrome and sarcopenia. Nutrients *13*, 3519. https://doi.org/10.3390/nu13103519.
5. Paul, P.K., and Kumar, A. (2011). TRAF6 coordinates the activation of autophagy and ubiquitin-proteasome systems in atrophying skeletal muscle. Autophagy *7*, 555–556. https://doi.org/10.4161/auto.7.5.15102.
6. Mizushima, N., and Komatsu, M. (2011). Autophagy: Renovation of cells and tissues. Cell *147*, 728–741. https://doi.org/10.1016/j.cell.2011.10.026.
7. Ge, Y., Huang, M., and Yao, Y.M. (2018). Autophagy and proinflammatory cytokines: Interactions and clinical implications. Cytokine Growth Factor Rev. *43*, 38–46. https://doi.org/10.1016/j.cytogfr.2018.07.001.
8. Haddad, F., Zaldivar, F., Cooper, D.M., and Adams, G.R. (2005). IL-6-induced skeletal muscle atrophy. J. Appl. Physiol. *98*, 911–917. https://doi.org/10.1152/japplphysiol.01026.2004.
9. Zamir, O., Hasselgren, P.O., O'Brien, W., Thompson, R.C., and Fischer, J.E. (1992). Muscle protein breakdown during endotoxemia in rats and after treatment with interleukin-1 receptor antagonist (IL-1RA). Ann. Surg. *216*, 381–385. , discussion 386-7. https://doi.org/10.1097/00000658-199209000-00018.
10. Qin, B., Zhou, Z., He, J., Yan, C., and Ding, S. (2015). IL-6 inhibits starvation-induced autophagy via the STAT3/Bcl-2 signaling pathway. Sci. Rep. *5*, 15701. https://doi.org/10.1038/srep15701.
11. Huang, Z., Zhong, L., Zhu, J., Xu, H., Ma, W., Zhang, L., Shen, Y., Law, B.Y.K., Ding, F., Gu, X., and Sun, H. (2020). Inhibition of IL-6/JAK/STAT3 pathway rescues denervation-induced skeletal muscle atrophy. Ann. Transl. Med. *8*, 1681. https://doi.org/10.21037/atm-20-7269.
12. Zanders, L., Kny, M., Hahn, A., Schmidt, S., Wundersitz, S., Todiras, M., Lahmann, I., Bandyopadhyay, A., Wollersheim, T., Kaderali, L., et al. (2022). Sepsis induces interleukin 6, gp130/JAK2/STAT3, and muscle wasting. J. Cachexia Sarcopenia Muscle *13*, 713–727. https://doi.org/10.1002/jcsm.12867.
13. Yamada, E., Bastie, C.C., Koga, H., Wang, Y., Cuervo, A.M., and Pessin, J.E. (2012). Mouse

skeletal muscle fiber-type-specific macroautophagy and muscle wasting are regulated by a Fyn/STAT3/Vps34 signaling pathway. Cell Rep. *1*, 557–569. https://doi.org/10.1016/j.celrep.2012.03.014.

14. Hallek, M., Neumann, C., Schäffer, M., Danhauser-Riedl, S., Von Bubnoff, N., De Vos, G., Druker, B.J., Yasukawa, K., Griffin, J.D., and Emmerich, B. (1997). Signal transduction of interleukin-6 involves tyrosine phosphorylation of multiple cytosolic proteins and activation of Src-family kinases Fyn, Hck, and Lyn in multiple myeloma cell lines. Exp. Hematol. *25*, 1367–1377.
15. Ju, J.S., Varadhachary, A.S., Miller, S.E., and Weihl, C.C. (2010). Quantitation of 'autophagic flux' in mature skeletal muscle. Autophagy *6*, 929–935. https://doi.org/10.4161/auto.6.7.12785.
16. Masiero, E., Agatea, L., Mammucari, C., Blaauw, B., Loro, E., Komatsu, M., Metzger, D., Reggiani, C., Schiaffino, S., and Sandri, M. (2009). Autophagy is required to maintain muscle mass. Cell Metab. *10*, 507–515. https://doi.org/10.1016/j.cmet.2009.10.008.
17. Yakabe, M., Ogawa, S., Ota, H., Iijima, K., Eto, M., Ouchi, Y., and Akishita, M. (2018). Inhibition of interleukin-6 decreases atrogene expression and ameliorates tail suspension-induced skeletal muscle atrophy. PLoS One *13*, e0191318. https://doi.org/10.1371/journal.pone.0191318.
18. Kachaeva, E.V., and Shenkman, B.S. (2012). Various jobs of proteolytic enzymes in skeletal muscle during unloading: Facts and speculations. J. Biomed. Biotechnol. *2012*, 493618. https://doi.org/10.1155/2012/493618.
19. Bodine, S.C., Latres, E., Baumhueter, S., Lai, V.K., Nunez, L., Clarke, B.A., Poueymirou, W.T., Panaro, F.J., Na, E., Dharmarajan, K., et al. (2001). Identification of ubiquitin ligases required for skeletal muscle atrophy. Science *294*, 1704–1708. https://doi.org/10.1126/science.1065874.
20. Klionsky, D.J., Abdelmohsen, K., Abe, A., Abedin, M.J., Abeliovich, H., Acevedo Arozena, A., Adachi, H., Adams, C.M., Adams, P.D., Adeli, K., et al. (2016). Guidelines for the use and interpretation of assays for monitoring autophagy (3rd Edition). Autophagy *12*, 1–222. https://doi.org/10.1080/15548627.2015.1100356.
21. Linden, D.C., Newton, M.W., Grinnell, A.D., and Jenden, D.J. (1983). Rapid decline in acetylcholine release and content of rat extensor digitorum longus muscle after denervation. Exp. Neurol. *81*, 613–626. https://doi.org/10.1016/0014-4886(83)90330-8.
22. Klionsky, D.J., Abdalla, F.C., Abeliovich, H., Abraham, R.T., Acevedo-Arozena, A., Adeli, K., Agholme, L., Agnello, M., Agostinis, P., Aguirre-Ghiso, J.A., et al. (2012). Guidelines for the use and interpretation of assays for monitoring autophagy. Autophagy *8*, 445–544. https://doi.org/10.4161/auto.19496.
23. Malicdan, M.C.V., Noguchi, S., and Nishino, I. (2009). Monitoring autophagy in muscle diseases. Methods Enzymol. *453*, 379–396. https://doi.org/10.1016/S0076-6879(08)04019-6.
24. Teng, B.T., Pei, X.M., Tam, E.W., Benzie, I.F., and Siu, P.M. (2011). Opposing responses of apoptosis and autophagy to moderate compression in skeletal muscle. Acta Physiol. *201*, 239–254. https://doi.org/10.1111/j.1748-1716.2010.02173.x.
25. Mitchell, W.K., Williams, J., Atherton, P., Larvin, M., Lund, J., and Narici, M. (2012). Sarcopenia, dynapenia, and the impact of advancing age on human skeletal muscle size and strength; a quantitative review. Front. Physiol. *3*, 260. https://doi.org/10.3389/fphys.2012.00260.
26. Christian, C.J., and Benian, G.M. (2020). Animal models of sarcopenia. Aging Cell *19*, e13223. https://doi.org/10.1111/acel.13223.
27. Xie, W.Q., He, M., Yu, D.J., Wu, Y.X., Wang, X.H., Lv, S., Xiao, W.F., and Li, Y.S. (2021). Mouse models of sarcopenia: classification and evaluation. J. Cachexia Sarcopenia Muscle *12*, 538–554. https://doi.org/10.1002/jcsm.12709.
28. Smith, C.L., Mittaud, P., Prescott, E.D., Fuhrer, C., and Burden, S.J. (2001). Src, fyn, and yes are not required for neuromuscular synapse formation but are necessary for stabilization of agrin-induced clusters of acetylcholine receptors. J. Neurosci. *21*, 3151–3160. https://doi.org/10.1523/JNEUROSCI.21-09-03151.2001.
29. Kadoguchi, T., Shimada, K., Miyazaki, T., Kitamura, K., Kunimoto, M., Aikawa, T., Sugita, Y., Ouchi, S., Shiozawa, T., Yokoyama-Nishitani, M., et al. (2020). Promotion of oxidative stress is associated with mitochondrial dysfunction and muscle atrophy in aging mice. Geriatr. Gerontol. Int. *20*, 78–84. https://doi.org/10.1111/ggi.13818.
30. You, J.S., Singh, N., Reyes-Ordonez, A., Khanna, N., Bao, Z., Zhao, H., and Chen, J. (2021). ARHGEF3 regulates skeletal muscle regeneration and strength through autophagy. Cell Rep. *34*, 108594. https://doi.org/10.1016/j.celrep.2020.108594.
31. Nascimbeni, A.C., Fanin, M., Masiero, E., Angelini, C., and Sandri, M. (2012). Impaired autophagy contributes to muscle atrophy in glycogen storage disease type II patients. Autophagy *8*, 1697–1700. https://doi.org/10.4161/auto.21691.
32. Li, C.W., Yu, K., Shyh-Chang, N., Li, G.X., Jiang, L.J., Yu, S.L., Xu, L.Y., Liu, R.J., Guo, Z.J., Xie, H.Y., et al. (2019). Circulating factors associated with sarcopenia during ageing and after intensive lifestyle intervention. J. Cachexia Sarcopenia Muscle *10*, 586–600. https://doi.org/10.1002/jcsm.12417.
33. Michaud, M., Balardy, L., Moulis, G., Gaudin, C., Peyrot, C., Vellas, B., Cesari, M., and Nourhashemi, F. (2013). Proinflammatory cytokines, aging, and age-related diseases. J. Am. Med. Dir. Assoc. *14*, 877–882. https://doi.org/10.1016/j.jamda.2013.05.009.
34. Muñoz-Cánoves, P., Scheele, C., Pedersen, B.K., and Serrano, A.L. (2013). Interleukin-6 myokine signaling in skeletal muscle: A double-edged sword? FEBS J. *280*, 4131–4148. https://doi.org/10.1111/febs.12338.
35. Pedersen, B.K., and Febbraio, M.A. (2008). Muscle as an endocrine organ: Focus on muscle-derived interleukin-6. Physiol. Rev. *88*, 1379–1406. https://doi.org/10.1152/physrev.90100.2007.
36. Vepachedu, R., Gorska, M.M., Singhania, N., Cosgrove, G.P., Brown, K.K., and Alam, R. (2007). Unc119 regulates myofibroblast differentiation through the activation of Fyn and the p38 MAPK pathway. J. Immunol. *179*, 682–690. https://doi.org/10.4049/jimmunol.179.1.682.
37. Seo, H.Y., Jeon, J.H., Jung, Y.A., Jung, G.S., Lee, E.J., Choi, Y.K., Park, K.G., Choe, M.S., Jang, B.K., Kim, M.K., and Lee, I.K. (2016). Fyn deficiency attenuates renal fibrosis by inhibition of phospho-STAT3. Kidney Int. *90*, 1285–1297. https://doi.org/10.1016/j.kint.2016.06.038.
38. Lee, T.W.A., Kwon, H., Zong, H., Yamada, E., Vatish, M., Pessin, J.E., and Bastie, C.C. (2013). Fyn deficiency promotes a preferential increase in subcutaneous adipose tissue mass and decreased visceral adipose tissue inflammation. Diabetes *62*, 1537–1546. https://doi.org/10.2337/db12-0920.
39. McKenna, C.F., and Fry, C.S. (2017). Altered satellite cell dynamics accompany skeletal muscle atrophy during chronic illness, disuse, and aging. Curr. Opin. Clin. Nutr. Metab. Care *20*, 447–452. https://doi.org/10.1097/MCO.0000000000000409.
40. Schneider, C.A., Rasband, W.S., and Eliceiri, K.W. (2012). NIH Image to ImageJ: 25 years of image analysis. Nat. Methods *9*, 671–675. https://doi.org/10.1038/nmeth.2089.
41. Faul, F., Erdfelder, E., Buchner, A., and Lang, A.G. (2009). Statistical power analyses using G*Power 3.1: Tests for correlation and regression analyses. Behav. Res. Methods *41*, 1149–1160. https://doi.org/10.3758/BRM.41.4.1149.
42. Yagi, T., Aizawa, S., Tokunaga, T., Shigetani, Y., Takeda, N., and Ikawa, Y. (1993). A role for Fyn tyrosine kinase in the suckling behaviour of neonatal mice. Nature *366*, 742–745. https://doi.org/10.1038/366742a0.
43. Savastano, L.E., Laurito, S.R., Fitt, M.R., Rasmussen, J.A., Gonzalez Polo, V., and Patterson, S.I. (2014). Sciatic nerve injury: A simple and subtle model for investigating many aspects of nervous system damage and recovery. J. Neurosci. Methods *227*, 166–180. https://doi.org/10.1016/j.jneumeth.2014.01.020.
44. Raices, M., Bukata, L., Sakuma, S., Borlido, J., Hernandez, L.S., Hart, D.O., and D'Angelo, M.A. (2017). Nuclear pores regulate muscle development and maintenance by assembling a localized Mef2C complex. Dev. Cell *41*, 540–554.e7. https://doi.org/10.1016/j.devcel.2017.05.007.
45. Baumann, C.W., Liu, H.M., and Thompson, L.V. (2016). Denervation-induced activation of the ubiquitin-proteasome system reduces skeletal muscle quantity not quality. PLoS One *11*, e0160839. https://doi.org/10.1371/journal.pone.0160839.

STAR★METHODS

KEY RESOURCES TABLE

REAGENT or RESOURCE	SOURCE	IDENTIFIER
Antibodies		
Mouse monoclonal antibody against Fyn (1:1000)	Abcam	ab1881; RRID:AB_2232153
Rabbit polyclonal antibody against Fyn (1:1000)	Santa Cruz Biotechnology	SC-16; RRID:AB_631528
Rabbit polyclonal antibodies against STAT3 (1:1000)	Cell Signaling	CS9132; RRID:AB_331588
Mouse monoclonal antibodies against pY705-STAT3 (1:1000)	Cell Signaling	CS9138S; RRID:AB_331262
Rabbit polyclonal antibody against pY705-STAT3 (1:1000)	Santa Cruz Biotechnology	SC7993R; RRID:AB_656684
Rabbit polyclonal antibody against LC3 (1:1000)	Novus Biotechnology Inc.	NB100-2331; RRID:AB_10001955
Mouse monoclonal antibody against GAPDH (1:10000)	MBL Co.	M171-3; RRID:AB_10597731
Chemicals, peptides, and recombinant proteins		
Leupeptin hemisulfate	Thermo Fisher Scientific	BP2662-25
IL-1	Thermo Fisher Scientific	10139HNAE5
IL6	Thermo Fisher Scientific	10395HNAE5
IL18	MBL Co., Ltd.	B003-5
Protease inhibitor cocktail	Sigma-Aldrich	535141
Critical commercial assays		
BCA Protein Assay Kit	Thermo Fisher Scientific	Cat# 23225
QIAzol Lysis Reagent	Qiagen	Cat# 79306
RNeasy Mini Kit	Qiagen	Cat# 74004
SuperScript VILO cDNA synthesis kit	Thermo Fisher Scientific	Cat# 11754050
Experimental models: Cell lines		
Non-target C2C12 myoblasts	ATCC	CRL-1772; RRID: CVCL_0188
Fyn-knockdown C2C12 myoblasts	This paper	N/A
Experimental models: Organisms/strains		
Male C57BL/6N mice	Charles River Laboratories	Animal Models | Charles River (criver.com)
pp59Fyn-knockout mice with a C57BL/6N background	RIKEN BioResource Research Center	https://mus.brc.riken.jp/ja/
Oligonucleotides		
Interleukin 6	Thermo Fisher Scientific	Mm00446190_m1
Atrogin-1	Thermo Fisher Scientific	Mm00499523_m1
MuRF-1	Thermo Fisher Scientific	Mm01185221_m1
ACTB	Thermo Fisher Scientific	Mm02619580_g1
Recombinant DNA		
MISSION shRNA lentivirus particle for Fyn	Merck	SHCLNG-NM_008054
Software and algorithms		
Image J	Schneider et al.[40]	https://imagej.nih.gov/ij/
G-Power	Faul et al.[41]	Universität Düsseldorf: G*Power (hhu.de)

RESOURCE AVAILABILITY

Lead contact

Information and requests for resources should be directed to and be fulfilled by the Lead Contact, Yamada Eijiro (eijiro.yamada@gunma-u.ac.jp).

Materials availability

This study did not generate new unique reagents.

Data and code availability

- All data reported in this paper will be shared by the lead contact upon request.
- This paper does not report original code.
- Any additional information required to reanalyze the data reported in this paper is available from the lead contact upon request.

EXPERIMENTAL MODEL AND SUBJECT DETAILS

Animals

All experiments were performed using male mice. For experiments with younger mice (8–12 weeks old) (Figure 1 and Figure S1), male C57BL/6N mice were obtained from Charles River Laboratories (Wilmington, MA, USA). pp59^{Fyn}-knockout mice with a C57BL/6N background (RBRC1000) were obtained from RIKEN BioResource Research Center (Tsukuba, Japan).[42] All homozygous and control mice were obtained by crossing heterozygous mice. Animals were housed in a facility equipped with a 12 h light/dark cycle and given *ad libitum* access to standard chow containing 67% carbohydrate, 19% protein, and 4% fat. Mice were randomly assigned to experimental and control groups. Prior to the experiment, adjustments were made to ensure that there were no differences in body weight between the groups. The investigators were not blinded to experimental vs. control mice, as the experimental mice were thinner due to muscle loss. In each experiment, all animals completed the protocol; no mice were excluded. All studies were approved and performed in compliance with the guidelines of the Review Committee on Animal Use at Gunma University, Maebashi, Japan (Approval No. 17-070).

Sciatic denervation model

Sciatic denervation was performed as previously described.[43] Briefly, anesthesia was administered using 5% isoflurane and 1 L/min oxygen flow and was maintained with 2% isoflurane. The sciatic nerve in the left hind limb was cut. The sciatic nerve in the right hind limb was exposed in the same manner but was not cut (sham denervation). The surgery was performed on three male mice under the same conditions. After the operation, the mice were housed under the same conditions for two weeks. Euthanasia by cervical dislocation was then performed before harvesting the muscles.

TS model

Mice were subjected to TS as described previously.[17] Briefly, the tail was suspended from the top of the cage such that the animal was not able to use the lower limbs but could only use the upper limbs to move around. Six male mice were placed in the tail-suspension cage using the same method. Tail-suspended mice were housed under the same conditions for two weeks. Euthanasia by cervical dislocation was then performed before harvesting the muscles.

In vivo assay for autophagy flux

An *in vivo* assay for autophagy flux in the tail-suspension model was performed using colchicine, as described previously.[15] Briefly, 0.4 mg/kg/day of colchicine was injected intraperitoneally into three male mice during the last two days of the experiment (48 h and 24 h before euthanasia). As controls, three other male mice were administered saline intraperitoneally. The mice were starved for 30 h before the last colchicine (or saline) dose and then euthanized by cervical dislocation before the muscles were harvested.

Cell culture and generation of C2C12 myotubes with Fyn knockdown

Non-target C2C12 (RRID: CVCL_0188) and Fyn-knockdown C2C12 myoblasts were cultured in Dulbecco's Modified Eagle's Medium (DMEM, Invitrogen, CA, USA) containing 20% fetal bovine serum (FBS, Atlanta Biologicals, Flowery Branch, GA, USA) and induced to differentiate into myotubes using 2% calf serum. C2C12 myotubes were serum-starved for 2 h, followed by treatment with 10 ng/ml IL-1β, 20 ng/ml IL-6, and 10 ng/ml IL-8 for 15 min each at 37°C. Cells were incubated at 37°C in a humidified incubator with 5% CO_2. C2C12 myotubes expressing shRNA for Fyn were generated as follows: 50% confluent C2C12 myoblasts (ATCC, Manassas, VA, USA) were infected with MISSION shRNA lentivirus particle for Fyn (Merck, Burlington, MA, USA), followed by selection with 5 μg/ml puromycin. Selected single C2C12 myoblasts were cloned on a 96-well plate and screened for Fyn expression.[44]

METHOD DETAILS

Antibodies and reagents

Mouse monoclonal antibody against Fyn and rabbit polyclonal antibody against Fyn were purchased from Abcam (Cambridge, MA, USA) and Santa Cruz Biotechnology (Santa Cruz, CA, USA), respectively. Rabbit polyclonal antibodies against STAT3 and pY705-STAT3 were obtained from Cell Signaling (Boston, MA, USA) and rabbit polyclonal antibody against pY705-STAT3 was obtained from Santa Cruz Biotechnology (Santa Cruz, CA, USA). Anti-LC3 rabbit polyclonal antibody was obtained from Novus Biotechnology Inc. (Littleton, CO,

USA). Anti-GAPDH mouse monoclonal antibody was obtained from MBL Co., Ltd. (Nagoya, Japan). Leupeptin hemisulfate, IL-1, and IL6 were purchased from Thermo Fisher Scientific (Pittsburgh, PA, USA) and IL18 was purchased from MBL Co., Ltd. (Nagoya, Japan). All other reagents were purchased from Merck (Burlington, MA, USA). The dilutions and catalog numbers of antibodies used are stated in the key resources table.

Western blotting and immunoprecipitation

Western blotting

Mice were euthanized by cervical dislocation, and the skeletal muscles in the lower limbs were immediately dissected. Soleus, gastrocnemius, EDL, TA, and quadricep muscles were collected in this order. After weighing, the dissected muscles were frozen in liquid nitrogen and stored at −80°C. Western blotting was performed on gastrocnemius and TA muscles (see Figures 1, 4, 5, and 6 for details). Frozen muscles were homogenized using a Bead beater homogenizer (Beads crusher μT-12, Taitec Co., Tokyo, Japan) in 0.4 ml of ice-cold NP40 lysis buffer (25 mM Tris-HCl, pH 7.2; 1% NP40; 10% glycerol; 50 mM NaF; 10 mM $Na_4P_2O_7 \cdot 10H_2O$; 135 mM NaCl; 1 mM Na_3VO_4) containing a protease inhibitor cocktail (Sigma-Aldrich, St. Louis, MO, USA) in 0.5-ml screw-cap tubes on ice. The skeletal muscle homogenate was then centrifuged at 15,000 rpm for 10 min at 4°C. Protein concentration was measured using the bicinchoninic acid (BCA) Protein Assay Kit (Thermo Fisher Scientific, Waltham, MA, USA). Protein (50 μg) was separated onto 8–15% SDS-PAGE gels, followed by transfer to PVDF membranes (Bio-Rad, Hercules, CA, USA). Transferred membranes were blocked with 5% non-fat milk in Tris-buffered saline containing 0.5% Tween-20 (TBS-T) before exposure to primary antibodies. Membranes were incubated with primary antibodies and blots were subsequently incubated with peroxidase-conjugated secondary antibodies. Immunoreactive proteins were revealed using ECL Plus (Thermo Fisher Scientific, Waltham, MA, USA).

Immunoprecipitation

Lysates were prepared in 0.4 ml of ice-cold NP40 lysis buffer containing a protease inhibitor cocktail (Sigma-Aldrich, St. Louis, MO, USA). Homogenates were centrifuged for 30 min at 14,000 rpm at 4°C and supernatants were collected. Protein concentration was determined using the BCA Protein Assay Kit (Thermo Fisher Scientific, Waltham, MA, USA). Lysates (5–6 mg) were immunoprecipitated using the indicated antibodies, followed by incubation with Protein A/G Plus (Santa Cruz Biotechnology, Santa Cruz, CA, USA). Samples were washed three times, boiled, and separated on 10% SDS-PAGE gels, followed by an overnight transfer. Western blot analysis was performed with the indicated antibodies.

Quantitative PCR analysis

Frozen gastrocnemius muscle samples were homogenized with QIAzol Lysis Reagent (Qiagen, Valencia, CA, USA) using the Bead beater homogenizer (Taitec Co., Tokyo, Japan). Total RNA was extracted using the RNeasy Mini Kit (Qiagen, Valencia, CA, USA), followed by reverse transcription to cDNA using the Super Script VILO cDNA synthesis kit (Thermo Fisher Scientific, Waltham, MA, USA). Relative mRNA expression levels were quantified using TaqMan RT-PCR (Thermo Fisher Scientific, Waltham, MA, USA) detailed in the key resources table. Samples were adjusted for total mRNA content by comparison with beta-actin expression with identical C(T) values between WT and Fyn-knockout mice. Relative mRNA expression levels were determined using the 2-ΔΔCT method. All primer-probe mixtures were obtained from Applied Biosystems (Branchburg, NJ, USA).

Tissue preparation for histology

Resected muscles were frozen in 2-methylbutane, cooled in liquid nitrogen, and stored at -80°C. Transverse serial sections were stained with H&E, COX, SDH, periodic acid-Schiff (PAS), SERCA 1, SERCA 2, and NADH-TR. Section preparation and staining of frozen specimens were performed by Sept Sapie (Mizuho, Tokyo, Japan). Immunofluorescence was performed using a p62 guinea pig polyclonal antibody, followed by Alexa Fluor 594 anti-guinea pig IgG. The samples were mounted on glass slides with Prolong Gold anti-fade reagent and DAPI (Invitrogen, Waltham, MA, USA). The cells were imaged using a confocal fluorescence microscope (TCS SP5 confocal; Leica Microsystems, Wetzlar, Germany).

QUANTIFICATION AND STATISTICAL ANALYSIS

Quantification

Quantitative evaluation of western blotting was performed using ImageJ (1.53).[40] A rectangular ROI containing the bands was set up, and the ROI of an identical size was used for all the evaluated lanes. The pixel values were calculated and corrected with the pixel values of the control, and the corrected pixel values were compared for each lane to evaluate the protein expression level. Using the results of three representative blots, the mean value was calculated and analyzed using the Mann–Whitney U test.

Statistics

Power analysis

Based on a previous report,[45] the effective size was calculated as d = 1.69 using soleus muscle weight measurements (control group: mean 10.76 μg, SD 2.28; denervated muscle group: mean 7.72 μg, SD 1.12). The number of samples required was calculated with an α of 0.05 and power of 0.8; six samples were determined to be needed for each group. G-power (3.1.9.2)[41] was used to calculate the sample size.

Statistical analyses

All data are presented as the mean $\pm$ standard error of the mean. Data with p-values < 0.05 were considered statistically significant and were determined using the Mann–Whitney U test for western blotting results and the Student's t-test for qPCR results and muscle fiber size analysis.